Nuclear Instruments and Methods in Physics Research A 597 (2008) 61–66

Contents lists available at ScienceDirect

Nuclear Instruments and Methods in Physics Research A

journal homepage: www.elsevier.com/locate/nima

End-to-end absolute energy calibration of atmospheric fluorescence telescopes by an electron linear accelerator

T. Shibata [a,*], A. Enomoto [b], S. Fukuda [b], M. Fukushima [a], K. Furukawa [b], D. Ikeda [a], M. Ikeda [b], K. Kakihara [b], S. Ohsawa [b], H. Sagawa [a], M. Satoh [b], T. Shidara [b], T. Sugimura [b], M. Yoshida [b]

[a] ICRR, University of Tokyo, 5-1-5 Kashiwanoha, Kashiwa, Chiba 277-8582, Japan
[b] High Energy Accelerator Research Organization, 1-1 Oho, Tsukuba, Ibaraki 305-0801, Japan

the Telescope Array Collaboration

ARTICLE INFO

Available online 22 August 2008

Keywords:
Cosmic ray
Fluorescence light
LINAC
End-to-end calibration

ABSTRACT

The Telescope Array (TA) is a hybrid detector composed of atmospheric fluorescence telescopes and a ground array of particle detectors for the precise energy measurement of ultra high-energy cosmic rays. We propose an end-to-end absolute energy calibration of fluorescence telescopes by using air showers induced by electron beams from a linear accelerator, which will be installed at the site of the TA experiment and will have a well-measured beam energy. We have simulated electron beam dynamics and interaction of electrons in air to evaluate the accuracy of the beam energy determination, beam currents, air showers, and detector response using a beam simulation code (PARMELA) and GEANT4. We found that the systematic error of energy measurement estimated for the TA fluorescence telescopes can be reduced from 23% to 17% by this end-to-end energy calibration. We are developing and constructing a compact linear accelerator with a maximum electron energy of 40 MeV and an intensity of 6.4 mJ/pulse. In this article, we describe the method of absolute energy calibration and the design of the accelerator.

1. Introduction

Ultra high-energy cosmic rays (UHECRs) are generated outside this Galaxy and propagate over long distances in the universe. We are trying to detect the UHECRs and to discover their origin and understand the process of their acceleration. The Akeno Giant Air Shower Array (AGASA), consisted of plastic scintillation counters and the High Resolution Fly's Eye (HiRes) experiment, applying the fluorescence technique detected UHECRs with energies greater than 10^{20} eV. The AGASA group reported an energy spectrum which extended beyond the Greisen–Zatsepin–Kuzmin (GZK) cutoff energy [1]. On the contrary, HiRes observed far fewer high events above the GZK-cutoff energy and a spectrum that was consistent with a GZK-cutoff. According to latest results of the AUGER experiment, the existence of the GZK-cutoff depression is supported [2]. To resolve this discrepancy, we constructed the Telescope Array (TA) observatory [3], which has a detection area of about 10 times larger than that of AGASA. TA consists of fluorescence detectors (FDs) and surface detectors, and is located in Utah, USA. In the TA experiment, we have three FD stations one of them consists of the HiRes-I telescopes. The FDs cooperate with the surface detector array on the cross-calibration of their systematic errors. The surface detector array consists of about 500 plastic scintillation counters which are deployed at intervals of 1.2 km over an area of about 700 km^2. We began observations in the summer of 2007.

The FDs observe air showers through the detections of ultraviolet photons which are emitted from nitrogen molecules, excited by air shower particles initiated by cosmic rays. The total number of generated fluorescence photons per unit depth along the shower axis is proportional to the energy deposit from charged particles in the shower which in turn is proportional to the energy of the primary cosmic ray. However, the fluorescence yield depends on the density, temperature, pressure, and humidity of the air. In addition, scattering and absorption during the transmission in the air reduce the flux of fluorescence photons. Thus, there is a large uncertainty in the primary energy measurement.

For example, the total systematic errors reported by the HiRes and the Pierre Auger experiments are 17% [4] and 22% [5], respectively. For the TA FDs, we estimated the total systematic error to be about 23%[1] [6,7], because the conventional method to estimate the primary energy is the conversion of ADC counts of

* Corresponding author.
E-mail address: shibata@icrr.u-tokyo.ac.jp (T. Shibata).

[1] Detail of the systematic error of the TA FDs are described in Section 6.

0168-9002/$ - see front matter © 2008 Published by Elsevier B.V.
doi:10.1016/j.nima.2008.08.048

each PMT by using many parameters such as fluorescence yield, mirror reflectivities, and so on. A large systematic error is caused by the multiplications of errors on the parameters which are individually calibrated. In order to avoid this difficulty, we will calibrate our telescopes with artificial air showers induced by calibration beams from an electron linear accelerator. The accelerator called TA-LINAC will be installed at the site of the TA experiment.

2. A new calibration of the energy measurement with fluorescence telescopes

We briefly describe the TA-LINAC and the calibration of the TA FDs. With this standard candle, we expect to calibrate all parameters which include fluorescence yield, mirror reflectivities, transparencies of filters, front acrylic panels, QE × CE (QE is quantum efficiency and CE is collection efficiency), and gain of PMT at the same time. On the other hand, we cannot calibrate atmospheric transparency and wavelength dependence of the detector response.

The TA-LINAC is compact in order to be installed into a shipping container, and to calibrate all of the fluorescence telescopes. The TA-LINAC will be installed 100 m away from one of the three FD stations. Therefore, we can neglect the extinction of the fluorescence photons in the air because the attenuation factor of fluorescence photons is about 1% for a distance of 100 m. It is not practical to locate the TA-LINAC farther than 100 m away from an FD station, because the LINAC would become much larger to provide sufficient output energy to cover the field of view (FOV) of the telescopes in elevation.

The basic specifications of the TA-LINAC are summarized in Table 1. For electrons, the main interaction process in air is ionization, because the critical energy in the air is 97 MeV. Practically, the energy deposit per particle through ionization loss will be about 0.2 MeV/m which is calculated by the Bethe–Bloch formula, and the energy deposit by bremsstrahlung will be about 0.1 MeV/m, the total it will be about 0.3 MeV/m. Thus, for a vertical shot of a 40 MeV beam the air shower will reach a height of about 130 m. Since the FOV of the telescopes at a distance of 100 m from the FD station is equivalent to 57 m in height, the electron beam leaves a trail on two imaging cameras of fluorescence telescopes.[2] The typical pulse width is set to 1 μs, because the typical pulse width of cosmic-ray events is 0.5 − 1.0 μs for a PMT with an FOV of 1°. The maximum repetition rate is 1 Hz. We can obtain the number of fluorescence photons in an air shower from one pulse shot with an accuracy sufficient for the energy calibration. Furthermore, we avoid the activation of the air by the electron beam. We compare the fluorescence photon flux from electron beams of the TA-LINAC with that from UHECR air showers. First, we should remember the fluorescence yield per particle is approximately proportional to its energy loss through electromagnetic interactions. For an electron beam, the total energy loss is equal to the total energy loss of the beam, $40\ \text{MeV} \times 10^9 = 4 \times 10^{16}$ eV, because the major energy loss of electrons is ionization. On the other hand, for UHECR air showers, the main components are electrons, positrons, and gamma rays. The typical energy of the electron component is about 100 MeV. Therefore the major energy loss process is also ionization and the total energy is of the order of 10^{20} eV. As a result, the fluorescence photon flux with 4×10^{16} eV energy deposit in the air at a distance of 100 m from the FD station is equivalent to that of 10^{20} eV energy deposit at a distance of 10 km. Thus, electron beams can be used as pseudo-cosmic-ray events.

Table 1
The basic specifications of the TA-LINAC

Beam energy	40 MeV
Output current	10^9 e$^-$/pulse
Beam intensity	6.4 mJ/pulse
Pulse width	2 μs (typical 1 μs)
Repetition rate	1 Hz

All values are maximum values and it is possible to continuously adjust them.

Furthermore, when comparing the TA-LINAC electron beam to a cosmic-ray shower, we must also consider the image length on the camera for each type of air shower. The electron beam from the TA-LINAC reaches a height of about 130 m above the ground. Then, the almost entire track of the beam is detected by the FD station, because the FOV of the station is 3 − 34° in elevation, and it is equivalent to 10–70 m at a distance of 100 m from the station. On the other hand, for an UHECR shower with 10^{20} eV energy, the average first interaction point is about 21–22 km a.s.l. and the shower maximum is estimated about 1.8–2.1 km a.s.l. [8,9]. Thus, we can observe the air shower around the UHECR shower maximum, because the station FOV is equivalent to 0.5–6 km a.s.l. at a distance of 10 km.

In addition to the discussions above, we have to remember the attenuation of fluorescence photons due to scattering in the air for cosmic-ray events. The number of photons is reduced during 10 km propagation. On the other hand, the effect of attenuation on the TA-LINAC beam is negligible, because we estimate the attenuation to be about 1–2%.

There is a plan to calibrate the wavelength dependence of detector response and attenuation coefficient between the TA-LINAC position and an FD station with a small multi-wavelength laser system which can be moved and be located at the TA-LINAC position for a more accurate energy calibration. If we shoot off the electron beam and laser beam at the same time, we can determine the attenuation coefficient and wavelength dependence of the detector response during the TA-LINAC operation. Thus, we can do a complementary and more accurate calibration with the TA-LINAC and the laser system.

3. Method for the energy calibration with the TA-LINAC

The energy calibration is performed by the comparison between the number of detected photons of real data and that of MC simulations (see e.g. Fig. 1) with the equation

$$R_i = \left(\frac{N_{\text{p.e.}}^{\text{DATA}}}{N_{\text{p.e.}}^{\text{MC}}} \right)_i \quad (i = 1 \ldots N_{\text{PMT}}) \tag{1}$$

where $N_{\text{p.e.}}^{\text{DATA}}$ and $N_{\text{p.e.}}^{\text{MC}}$ are the numbers of photo-electrons detected with the ith PMT in real data and MC simulation, respectively, and $N_{\text{PMT}}(= 256)$ is the number of PMTs in one telescope camera. The ideal value of R_i is "1", and we can correct $N_{\text{p.e.}}$ of the MC simulation with a calibration factor to modify these R_i. Here, we assume all R_i can be corrected with two calibration factors, f_{calib} and f_{bias} for one telescope, and it is defined by

$$y_i = f_{\text{calib}} \times x_i + f_{\text{bias}} \tag{2}$$

where y_i and x_i are defined by

$$y_i \equiv (N_{\text{p.e.}}^{\text{DATA}})_i \tag{3}$$

$$x_i \equiv (N_{\text{p.e}}^{\text{MC}})_i. \tag{4}$$

[2] In an FD station, the two telescopes are located in the vertical direction.

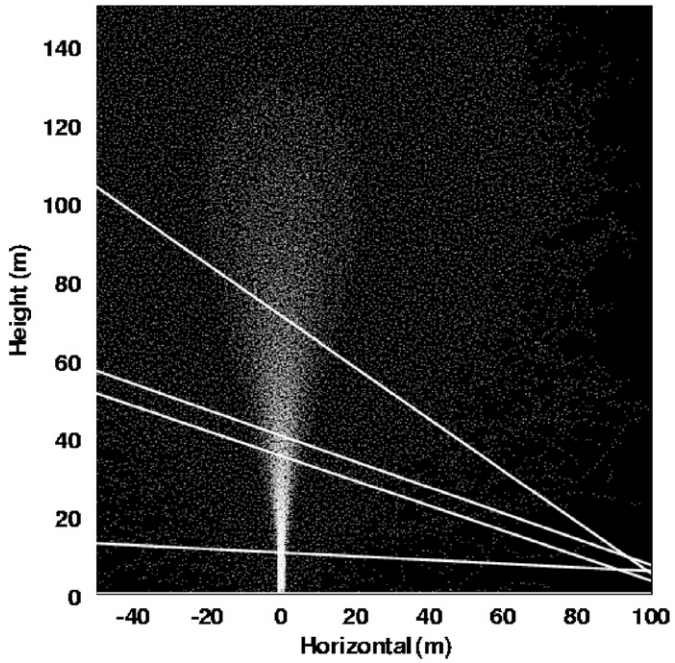

Fig. 1. An example of the simulated "air showers" induced by vertical beams of 40 MeV electrons ejected by the TA-LINAC with the GEANT4 code. Each white dot is a point where fluorescence photons are generated, and the solid lines show the field of view of the telescopes viewing higher and lower elevations [7].

$f_{\rm bias}$ is an offset value which is ideally zero. $f_{\rm calib}$ and $f_{\rm bias}$ are fitted with the least-square method as follows:

$$\begin{bmatrix} f_{\rm calib} \\ f_{\rm bias} \end{bmatrix} = \frac{1}{\Delta} \begin{bmatrix} \sum_i \frac{x_i^2}{\sigma_i^2} & -\sum_i \frac{x_i}{\sigma_i^2} \\ -\sum_i \frac{x_i}{\sigma_i^2} & \sum_i \frac{1}{\sigma_i^2} \end{bmatrix} \begin{bmatrix} \sum_i \frac{y_i}{\sigma_i^2} \\ \sum_i \frac{x_i y_i}{\sigma_i^2} \end{bmatrix} \tag{5}$$

$$\Delta \equiv \left(\sum_i \frac{x_i^2}{\sigma_i^2}\right) \times \left(\sum_i \frac{1}{\sigma_i^2}\right) - \left(\sum_i \frac{x_i}{\sigma_i^2}\right)^2. \tag{6}$$

The calibration factor is independent of any physical quantities such as incident electron energy, the number of detected photoelectrons, and properties of the PMTs. When $f_{\rm calib} \neq 1$, there are systematic uncertainties in the indices of reflection of the mirrors, transmission filters [14], or the QE, CE and gain of PMTs. We also consider the correlation between x_i and y_i. If we do not find linearity, there is the possibility that we have another systematic uncertainty which originates from the alignment of the system such as beam injection position, beam direction, the positions of the telescopes and their directions. We can calibrate these systematic uncertainties by comparing the distribution of $N_{\rm p.e.}^{\rm DATA}$ and that of $N_{\rm p.e.}^{\rm MC}$ in a telescope camera.

4. Fluorescence yield measurements with the TA-LINAC

As described in Section 2, we can calibrate all parameters at the same time, however, an independent measurement of the fluorescence yield with the TA-LINAC is very interesting. Previous experiments (the experiments by Nagano et al. [10], FLASH [11], MACFLY [12], and AIRFLY [13]) measured the absolute fluorescence yield as well as the dependence on environmental quantities such as temperature, pressure, relative humidity, and incident energy with electrons from radioactive sources or accelerators. The yields measured by these experiments have uncertainties larger than 10%.[3]

These experiments used a theoretical fluorescence yield formula for an ideal gas as follows:

$$\text{yield} = \sum_i \frac{dE}{dx} \frac{1}{RT} \frac{\Phi_i^0}{h\nu_i} \frac{p}{1 + p/p_i'} \tag{7}$$

where ν_i is the frequency and Φ_i^0 is the fluorescence efficiency of a photon from the i-th excited state of N_2. This formula includes temperature (T), pressure (p), energy deposit (dE/dx), and reference pressure (p_i'). The reference pressure depends upon the cross-sections of nitrogen–nitrogen and nitrogen–oxygen collisional de-excitation [10]. Recently, the importance of a temperature dependence of these cross-sections was pointed out [13,15]. Furthermore the relative humidity becomes to be a very important quantity, because it has a large influence on the fluorescence yield. The fluorescence yield under 100% relative humidity is 20% smaller than that under 0% [15]. Thus, we have to consider the dependence on temperature, pressure, and relative humidity seriously in our energy calibration with the TA-LINAC, and we have a proposal for the measurement of absolute fluorescence yield.

First, we consider the effect of temperature, pressure, and relative humidity in this calibration. Around the site of the TA experiment, the variation of temperature is about $\pm 30^\circ$ in one year. This is expected to result in a $\pm 5\%$ variation in the fluorescence yield. The variation of air pressure is about ± 20 hPa, the expected effect on the fluorescence yield is $\pm 2\%$ [7]. The relative humidity varies from about 10% to 100% in a year [16], we expect that the fluorescence yield will vary by about $\pm 10\%$.

Finally, we note that it is important to measure the absolute fluorescence yield with some PMTs and the yield of multi-wavelength with spectrometers which are installed in a chamber and are located around the injection position. We expect that the chamber can be used not only for the measurement of the fluorescence yield but also to monitor the output beam current.

5. A linear accelerator system

The development of the TA-LINAC began in April 2005 at the High Energy Accelerator Research and Organization (KEK) in Japan. We designed the TA-LINAC compactly for transportation, we also prepared a generator and a water cooling system because of the isolated operations of the accelerator. The construction work is continued by the end of 2007. Initial beam test will be performed at KEK in early 2008. Soon after that, the beam line and RF system will be packed in a 40-ft long shipping container and it will be installed at the TA site in Utah, USA. Fig. 2 is an illustration of the TA-LINAC. It consists of an electron gun, a prebuncher, a buncher, a main 2-m accelerator tube, a magnetic lens, Helmholtz coils, a set of doublet type quadrupole magnets for focusing the electron beam, a 90° bending magnet, a slit collimator, a high power S-band (2856 MHz) klystron, and a high power pulse modulator. A feature of the TA-LINAC is that we recycled old or spare components. Almost all the components are equipment of the KEK accelerator removal for the upgrade, and the high power pulse modulator was developed for the C-band Linear Collider system in KEK [17].

The electron gun is a thermal field emission type which has a dispenser cathode. It has a maximum peak current of 10 A. The saturation heater current is 2.4 A. We use a power supply which

[3] Recently, a measurement result whose uncertainty is about 5% was reported [14].

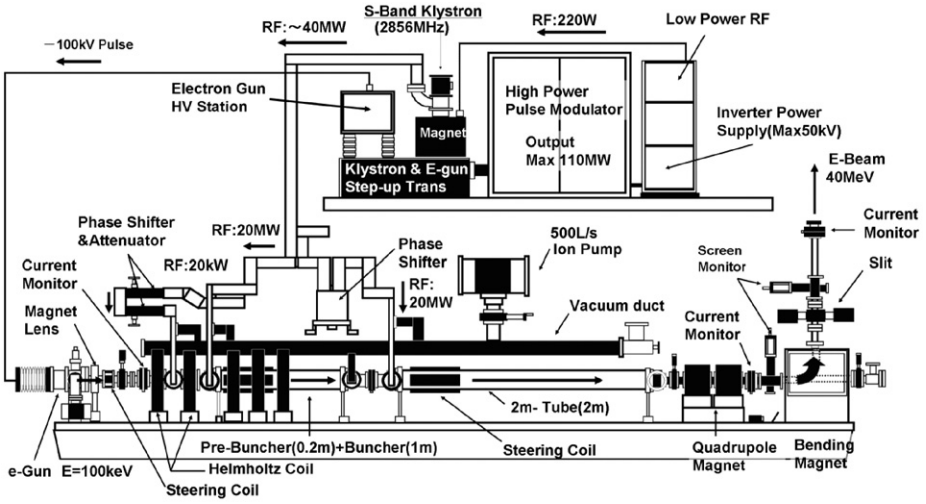

Fig. 2. Schematic view of the TA-LINAC.

can supply an output pulse of −100 kV, and that is the same device as the high power pulse modulator supplied for the RF system. The output current is controlled by adjusting the height of the grid pulse which is used as a trigger pulse, because the grid pulse is the voltage between the grid and the cathode.

The electron beam is focused by a magnetic lens with a maximum field strength of 1 kG. We prepared a small steering coil with a magnetic field of about 8 G. The 100 keV electrons are bent by 12 rad per 10 cm. The continuous electron beam which passes through the magnet lens is then broken into bunches by the prebuncher and buncher. They are given an RF structure with a period of 2856 MHz. The maximum accelerating gradients in the prebuncher and the buncher are 2 and 15 MV/m, respectively [18]. The maximum input power for them are 2 and 13 MW, respectively. The electron beam is accelerated in the main accelerator tube, which is an S-band, $2/3\pi$ mode Quasi-Constant Gradient type (made by MITSUBISHI Heavy Industries, Ltd.) with 54 cavities. Since its accelerating gain is 7.58 MV/$(\mathrm{MW})^{1/2}$ [19], the energy of electrons achieves the maximum of 40 MeV. We can control the output energy from 10 to 40 MeV continuously by using a phase shifter to adjust the initial input phase of RF to the accelerator tube.

We use magnets for focusing and bending electron beams. The main focusing magnet is a series of five Helmholtz coils. These are located in the buncher section. The maximum field strength is about 1 kG. We also use a doublet type quadrupole magnet for focusing the beam. It is installed at upstream of the bending magnet, and has a maximum field strength of 14 T/m. In order to adjust the beam direction, we installed steering coils not only just after the electron gun but also in the buncher and in the accelerator tube. These two coils have a maximum field strength of about 7 and 40 G, respectively. The direction of the electron beam is bent from the horizontal to the vertical with a bending magnet just after the quadrupole magnet. For 40 MeV electrons, the required field strength is 0.6 T, and thus the energy loss of an electron due to synchrotron radiation is 0.27 eV through the bending magnet, which is much smaller than 40 MeV. Finally the beam is collimated by a 50 mm thick slit, made of tantalum. We can determine the absolute energy within 1% for electrons with an energy of 40 MeV. For beam monitoring, we use a Faraday cup, four core monitors, and two screen monitors. The Faraday cup absolutely measures the beam charge. It includes a lead cup lined with carbon plates. The carbon plates suppress back scattering of the electrons. The core monitors measure relative beam current calibrated with the Faraday cup, and are installed at the outlets of the magnetic lens, the buncher tube, and the doublet type quadrupole magnet, and just in the upstream at the inlet of the output window. With the screen monitors at the inlet and the outlet of the bending magnet, we measure the profile of each beam, as well as its position and lateral spread, by observing fluorescence light when the electron beam collides with an alumina plate. We have installed two screen monitors just before and after the bending magnet.

The RF system consists of a high power pulse modulator, a step-up transformer, a high power S-band klystron (type PV-3030; made by MITSUBISHI-Denki), a 600 W output S-band RF source to input klystron, and waveguides.

The high power pulse modulator has a maximum power of 110 MW (22 kV × 5000 A) and a pulse width of about 2.5 μs. The output pulse of the modulator is transformed to a pulse of about 300 kV × 300 A by a step-up transformer for the input to a klystron. A part of the power is supplied to the electron gun. The maximum output power of the klystron is 40 MW and its micro-perveance is $I/V^{3/2}$∼2.0. The waveguides are made of oxygen-free copper and distribute high power RF to the prebuncher, the buncher, and the accelerator tube.

The estimated power consumption from the accelerator tubes, the waveguides, the klystron, and the magnets is about 10 kW in total. Thus, we have installed a cooling unit of 20 kW cooling power which uses 600 l of purified water. We estimate the maximum power consumption of the TA-LINAC system to be about 60 kW, and thus we will prepare a 100 kW electric generator. The RF system and the beam line are installed in a 40-ft long container. The cooling unit and the control units are installed in a 20-ft container. The gross weight of the 40-ft container and that of 20-ft container are about 20 ton, and about 5 ton, respectively.

6. Simulation of beam dynamics and interaction of electrons in air

We studied the electron beam dynamics, air showers generated by the beams, and the responses of the fluorescence telescopes by using PARMELA (Phase And Radial Motion in Electron Linear Accelerator) and GEANT4. PARMELA is a package for particle tracking simulation, which was developed at Los Alamos National Laboratory [20], and we used that for studying of transversal and longitudinal electron beam dynamics. We implemented the accelerator described above in PARMELA, and we

estimated the best input power of RF and relative phases for selecting the beam energy.

The dynamics of the electron beam in the doublet type quadrupole magnet, the bending magnet, and the slit were simulated with GEANT4. We determined the best width of the slit is 7 mm to achieve 1% accuracy of the beam energy. We also determined that the minimum required output power of the klystron is about 30 MW [7]. At the same time, we found that the ratio of the number of output electrons whose energy is 40 MeV to that of the injected ones from the electron gun is 0.51. Moreover, with the simulations we obtained energy spectra of electrons for several beam energy as shown in Fig. 3. Obviously, each distribution has a peak at the beam energy, but it also has a low-energy tail due to energy loss at the 100 μm thick stainless window. Because of this spectrum, the averaged beam energy is shifted by −2%, and the beam current increases by +1.5% due to interaction at the windows. The energies of secondary particles are smaller than 40 MeV and the total energy decreases by 0.7% only [7].

Interactions of 40 MeV electrons, the resulting fluorescence photons in air, and the responses of the telescopes were studied with GEANT4 based simulations. For these calculations, we adopted photon yield parameters which were measured by Nagano et al. [10] and we assumed the atmospheric composition to be 78.8% N_2 and 21.2% O_2. In this assumption, we neglect Ar, because the contribution of Ar is very small on fluorescence yield for 300–450 nm photons. We set up the injection position at 100 m distance and centered in the FOV of two telescopes. For one of the simulated beams, its longitudinal beam profile, i.e. the numbers of photons, and its image straddling two cameras are shown in Fig. 4. This result indicates that the shower maximum is about 60 m high and corresponds to about 0.2 radiation lengths.

Among the total number of generated fluorescence photons of 6.6×10^{11}, the number of photons detected with two cameras is 7.7×10^6 per pulse. Consequently, the maximum number of photons detected per PMT is estimated to be 1.6×10^5, which corresponds to 32,000 p.e.

The electron beams radiate not only fluorescence light, but also Cherenkov light because the critical energy of electrons which emit Cherenkov light in air is 21.15 MeV for a refraction index of the air of 1.0003. The number of emitted Cherenkov photons per electron is about 22/m for wavelengths between 300 and 450 nm. Unlike the isotropically emitted fluorescence photons, Cherenkov photons are emitted within 1.18° with respect to the trajectories of electrons.

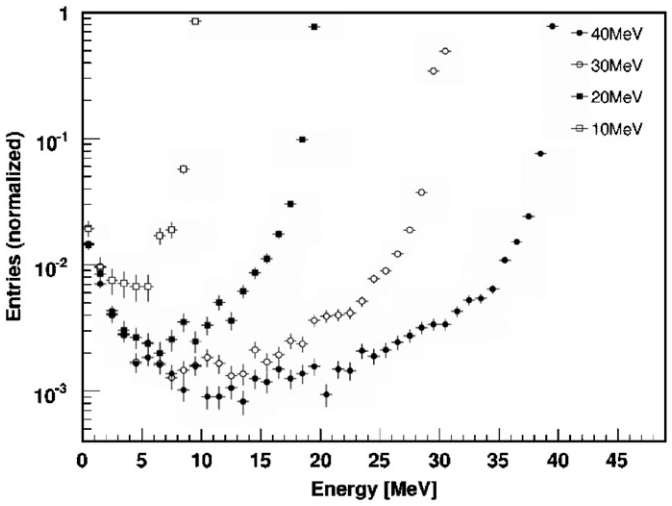

Fig. 3. The energy spectra of ejected electrons in beams with energies of 10, 20, 30, and 40 MeV, respectively [7].

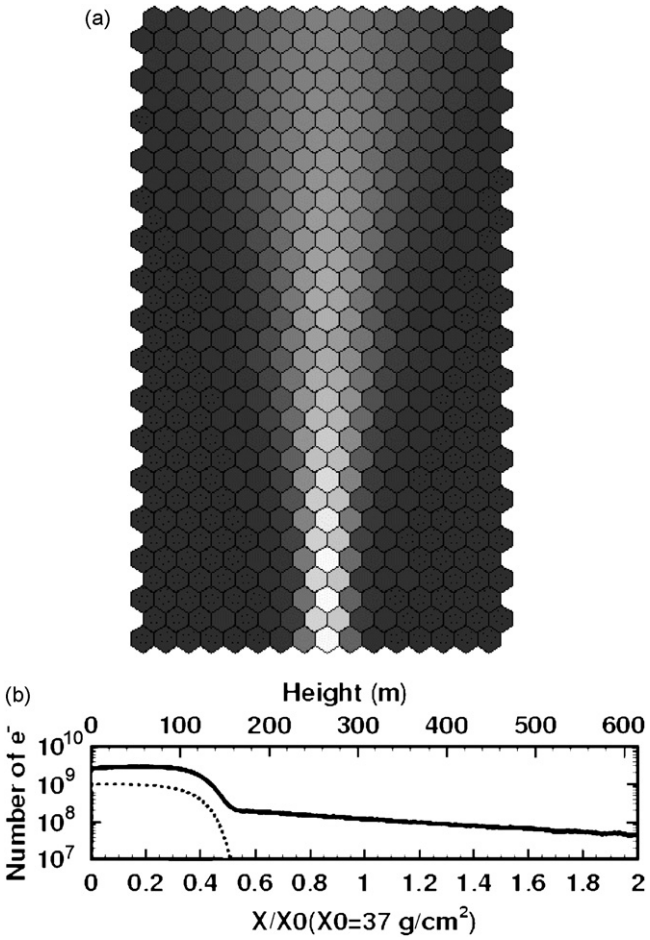

Fig. 4. (a) A simulated fluorescence image by a single shot from the accelerator with 40 MeV energy. (b) The longitudinal distribution of the number of electrons (dashed line is only primary electrons) in the shower shown in Fig. 4(a).

We considered two different contributions of the Cherenkov emission to the energy calibration by the TA-LINAC: Cherenkov light which enters the telescopes directly, and Cherenkov photons that are scattered into the telescopes.

For the direct case, when Cherenkov light is directly detected with a telescope, the electrons, which are sources of the light, must be scattered in the direction along the optical axis of the telescope before emitting the photons. Electrons are scattered through Coulomb scattering or Møller scattering. However, the cross-section of Coulomb backward scattering is about 10^{-6} that of forward scattering and the cross-section of Møller scattering is much smaller than that of Coulomb scattering. In addition, the solid angle from the scattered position to a telescope is about 10^{-5} sr. Accordingly, the number of electrons scattered in the direction of the optical axis is very small. Therefore, the contribution of Cherenkov light by scattered electrons is negligible. For the indirect case, the major process for scattering of light by air is Rayleigh scattering, while the Mie scattering is negligible. With detailed calculations, we found that the total number of Cherenkov photons detected directly and indirectly by two cameras is about 5×10^4 per pulse, and the maximum number of photons per PMT is about 1000 ph, which corresponds to 20 p.e./100 ns. This is smaller than 1% of the number of detected fluorescence photons and it is only twice the number of night sky background. Putting it all together, we can conclude that the influence of Cherenkov light on the energy calibration is negligible.

Using a simulation, we estimated the systematic uncertainties on the detected number of photons, taking into account the

Table 2
The summary of the systematic uncertainties TA FD and TA FD+TA-LINAC [6,7]

Source	TA FD (%)	TA FD + TA-LINAC (%)
Fluorescence yield	15	~8
Fluorescence telescope	10	~5
Atmospheric parameters	11	11
Reconstruction	6	6
Missing energy	5	5
Cherenkov flight	5	5
Total	23	~17

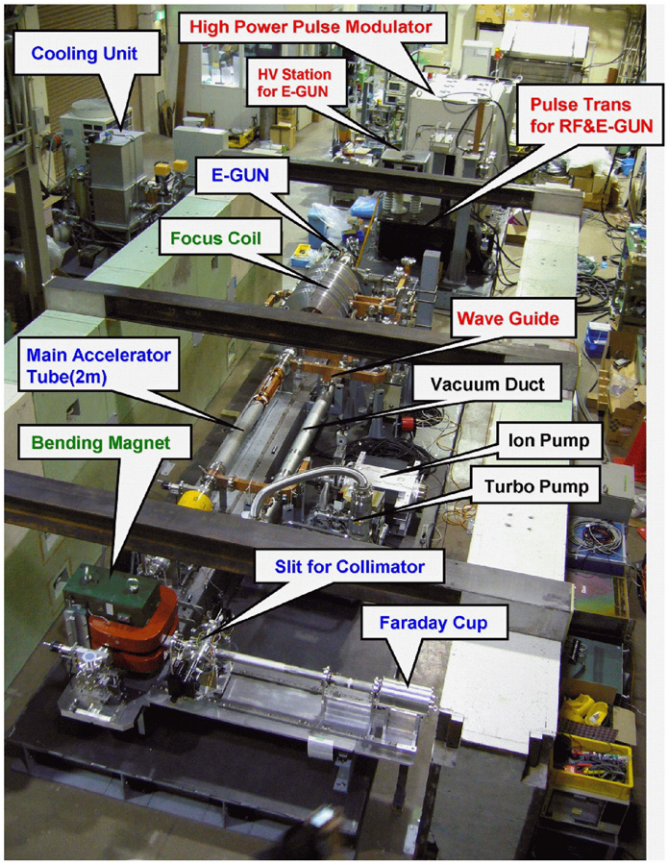

Fig. 5. A photograph of the constructed TA-LINAC at KEK. For beam tests at KEK, the beam is bent by 90° horizontally with a bending magnet.

uncertainties on the fluorescence yield, on telescope parameters except QE × CE, and gains of PMTs. In case of the fluorescence yield, we considered the errors of the fluorescence yield parameters and the variation of temperature and air pressure of three years at the TA site. However, since we will monitor the temperature and the pressure as described in Section 4, the systematic uncertainties due to these can be neglected. We also considered the uncertainties of the beam energy and the position of the container. As a result, the total uncertainty due to fluorescence yield was estimated to be ~8%. In case of the telescope parameters, we considered the errors of the mirror reflectivities, front acrylic panels, and filters. The uncertainty due to the telescope parameters was estimated to be ~5%. In Table 2, we summarize the uncertainties of the TA FD. The systematic uncertainties due to fluorescence yield, FD parameters, and atmospheric parameters are predominant. We expect that the total systematic uncertainty reduces from 23% to ~17% by the energy calibration with the TA-LINAC [7].

7. Construction and the prospects

In Fig. 5, we show a photo of the TA-LINAC under construction at KEK. All of the components for the beam line and RF waveguides were completed by the end of 2007. We also have done the RF system installation, performed RF performance tests, and we confirmed that the maximum output power from the klystron is 40 MW.

Furthermore we have installed the electron gun system and confirmed the electron beam of −100 kV and 300 mA with the core monitor. We will perform beam test at KEK after the completion of the accelerator, confirm the accuracy of the output beam energy and measure the beam current with a Faraday cup, which is located at the end of the beam line and some core monitors. At the same time, in order to determine the details concerning the necessary shielding at the TA site in Utah, we will measure the flux of gamma rays, X-rays, and neutrons around the beam line. After these tests at KEK, we will export the TA-LINAC to Utah. We will set the accelerator at our research site at Black Rock Mesa [6], and will start the operation in the spring of 2008.

8. Conclusion

The Telescope Array fluorescence telescopes will be the world's first air shower detectors which will be tried to be calibrated with an accelerator. In other words, we will use the electron linac beam as a source of absolute end-to-end energy calibration. Performance of the accelerator and responses of the telescopes were studied by using a beam simulation code (PARMELA) and GEANT4. The total systematic error of the energy measured with the fluorescence telescopes is estimated to be reduced from 23% to 17% by this calibration. The compact electron linac (TA-LINAC) is being developed and assembled at KEK in Japan and will be completed in early 2008. The beam operation of the TA-LINAC in Utah will start in spring of 2008.

Acknowledgments

The TA-LINAC work described in this article is supported by a Grant-in-Aid for Scientific Research (Kakenhi) "Absolute Calibration of the Fluorescence Telescopes for the Observation of the Highest Energy Cosmic Rays by a Compact Electron Accelerator" by the Ministry of Education, Culture, Sports, Science, and Technology of Japan, and by the Accelerator Science Synthesis Support Business by KEK. We gratefully acknowledge the supports from the staff of the KEK injector group, the KEKB group, and the technical staff of Mitsubishi Electric System and Service.

References

[1] K. Greisen, Phys. Rev. D 16 (1966) 748.
[2] K. Arisaka, et al., GAP Note 2004-037.
[3] M. Fukushima, et al, in: Proceedings of the 30th International Cosmic Ray Conference, Merida, Mexico, 2007, in press.
[4] G.B. Thomson, arXiv:astro-ph/0609403, 2006.
[5] B. Dawson, et al., arXiv:astro-ph/07061105v01, 2007.
[6] The Telescope Array Project Design Report, 2000.
[7] D. Ikeda, Master Thesis, University of Tokyo.
[8] K. Kasahara, private communication.
[9] M. Giorgio, arXi:astro-ph/08022214, 2008.
[10] M. Nagano, et al., Astropart. Phys. 22 (2004) 235.
[11] J. Belz, et al., Astropart. Phys. 25 (2006) 129.
[12] M. Colin, et al., Astropart. Phys. 27 (2007) 317.
[13] B. Buonomo, et al., Astropart. Phys. 28 (2007) 41.
[14] G. Lefeuvre, et al., Nucl. Instr. and Meth. A 578 (2007) 78.
[15] M. Ave, et al., arXiv:astro-ph/0711.4583v1, 2007.
[16] ⟨http://www.cemp.dri.edu/cemp/⟩.
[17] T. Shintake, et al., 25th Linear Accelerator Meeting in Japan, 2000, 12C-04.
[18] S. Ohsawa, in: Proceedings of PAC, vol. 93, 1993, p. 3087.
[19] I. Sato, Nucl. Instr. and Meth. 177 (1980) 91.
[20] L.M. Young, LANL Report No.LA-UR-96, 1996, p. 1835.